Supporting Information

Programmable Shrinking and Aggregation of pH-Thermo Dual-Responsive Amphiphilic Polymeric Nanoparticles Governed by Molecular Architecture

*Giuseppe Nunziata, Mattia Sponchioni * and Filippo Rossi **

Department of Chemistry, Materials and Chemical Engineering "Giulio Natta", Politecnico di Milano, piazza Leonardo da Vinci 32, 20133, Milan, Italy

* corresponding authors

E-mail: mattia.sponchioni@polimi.it
filippo.rossi@polimi.it

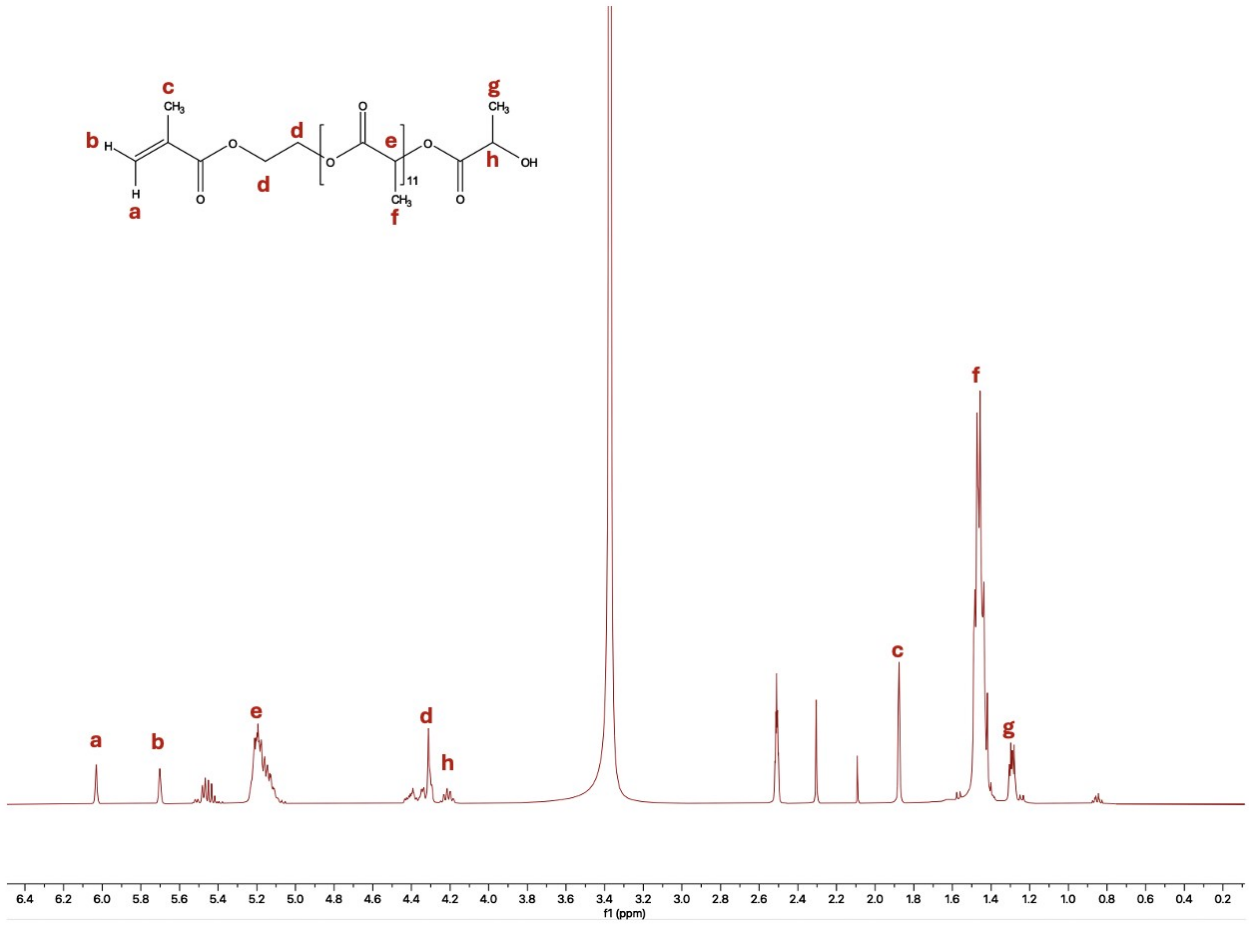

Figure S1. ^{1}H NMR spectrum of the HEMA-graft-LA$_{12}$ macromonomer (400 MHz, DMSO-d$_6$) with peak assignments. The characteristic signals of the PLA backbone (–CH– at ~5.2 ppm and –CH$_3$ at ~1.5 ppm) confirm the successful ring-opening polymerization of D,L-lactide. The presence of the vinyl protons of the methacrylate group (~6.1 and ~5.6 ppm) demonstrates the preservation of the polymerizable end-group, enabling subsequent RAFT chain extension. Signals in the 4.3–4.1 ppm region are attributed to the –O–CH$_2$– groups of the HEMA linker, further supporting the expected macromolecular structure.

^{1}H NMR (400 MHz, DMSO-d$_6$): δ (ppm) = 6.03 (a, CH$_2$=), 5.70 (b, CH=), 5.19 (e, –CH– PLA), 4.31 (d, –O–CH$_2$–), 4.21 (h, –CH–OH), 1.87 (c, =C–CH$_3$), 1.46 (f, –CH$_3$ PLA), 1.29 (g, –CH$_3$).

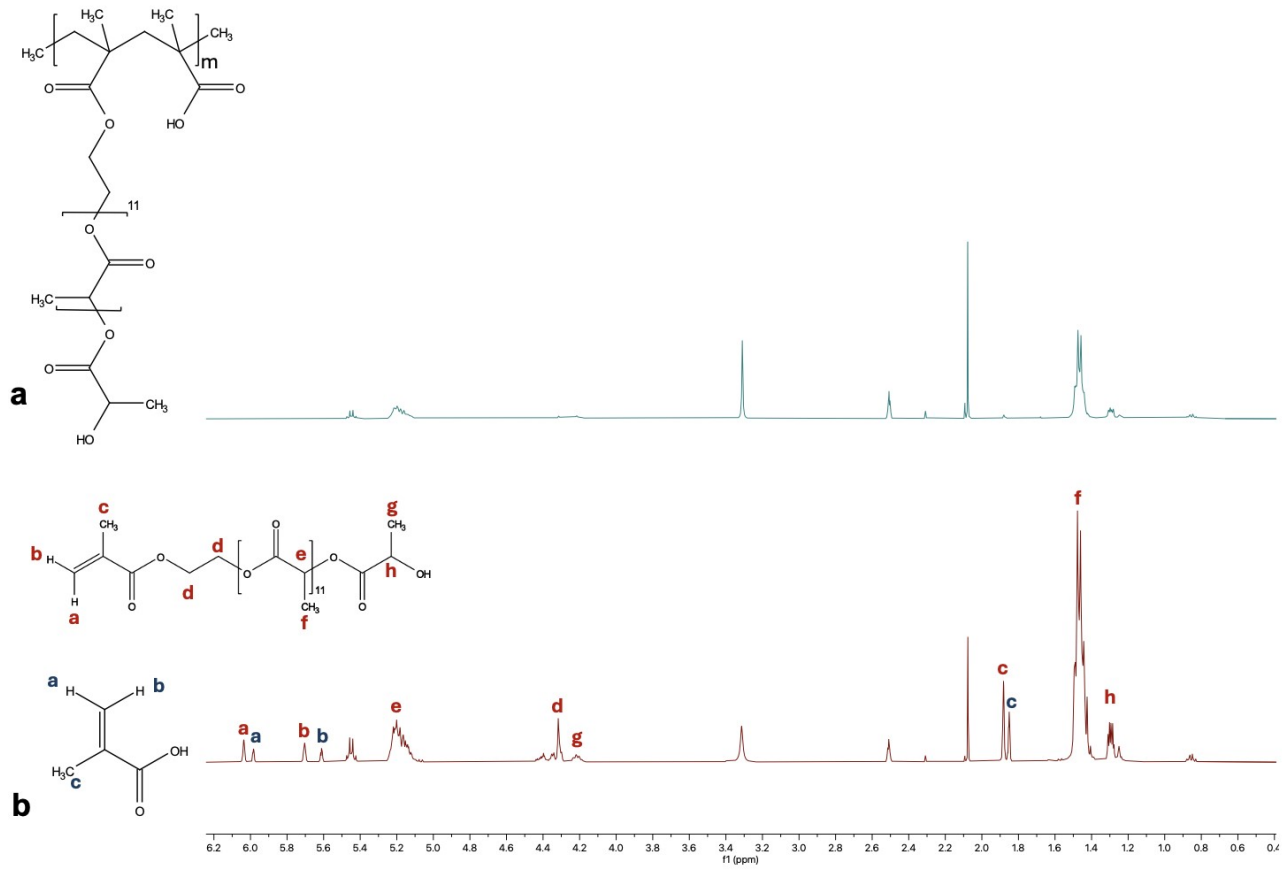

Figure S2. ^{1}H NMR spectra (400 MHz, DMSO-d_6) of the P((HEMA-graft-LA_{12})-co-MAA) copolymer compared with the corresponding monomers. **(a)** Final copolymer obtained after RAFT polymerization at 24 h. **(b)** Mixture of HEMA-graft-LA_{12} and methacrylic acid (MAA) monomers at 0h. The disappearance of the characteristic vinyl proton signals of the methacrylate groups (~6.0–5.5 ppm) in the copolymer spectrum confirms successful monomer conversion during the RAFT process. Concurrently, the appearance of broadened signals associated with the polymer backbone and side chains (e.g., PLA –CH– at ~5.2 ppm and –CH_3 at ~1.5 ppm) supports the formation of the statistical copolymer.

^{1}H NMR (400 MHz, DMSO-d_6): δ (ppm) = 6.03 (a (red), CH_2=), 5.98 (a (blue), CH=), 5.70 (b (red), CH=), 5.61 (b (blue), CH=), 5.19 (e, –CH– PLA), 4.31 (d, –O–CH_2–), 4.21 (h, –CH–OH), 1.87 (c (red), =C–CH_3), 1.81 (c (blue), =C–CH_3), 1.46 (f, –CH_3 PLA), 1.29 (g, –CH_3).

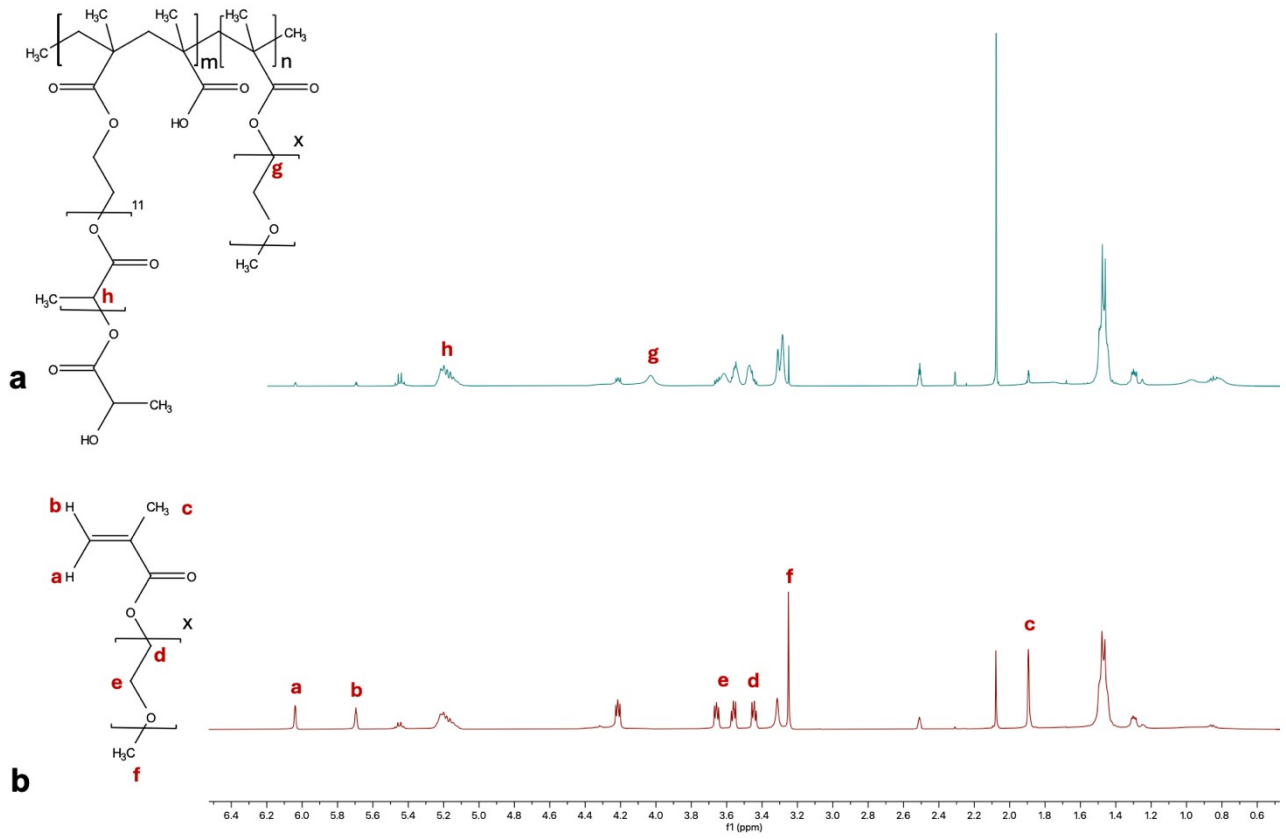

Figure S3. ^{1}H NMR spectra (400 MHz, DMSO-d_6) of the final P((HEMA-graft-LA_{12})-co-MAA)-b-P(EG_2MA-co-EG_8MA) block copolymer compared with the corresponding thermo-responsive monomers. (a) Final block copolymer obtained after RAFT chain extension. (b) Mixture of EG_2MA and EG_8MA monomers. The disappearance of the characteristic vinyl proton signals of the methacrylate groups (~6.0–5.5 ppm) in the copolymer spectrum confirms efficient monomer conversion during the chain extension step. The appearance of broad signals in the 4.2–3.5 ppm region, attributed to the oligo(ethylene glycol) side chains, together with the preserved signals of the PLA backbone (~5.2 and ~1.5 ppm), confirms the successful formation of the amphiphilic block copolymer. These spectral features demonstrate the effective incorporation of the thermo-responsive EGMA block while retaining the structural integrity of the initial macro-CTA.

^{1}H NMR (400 MHz, DMSO-d_6): δ (ppm) = 6.03 (a, CH_2=), 5.70 (b (red), CH=), 5.61 (b, CH=), 5.19 (h, –CH–PLA), 4,02 (g,–COO–CH_2–), 3.56 (e, –O–CH_2–), 3.44 (d,–CH_2–O), 3.25 (f, –CH–OH), 1.89 (c, =C–CH_3).

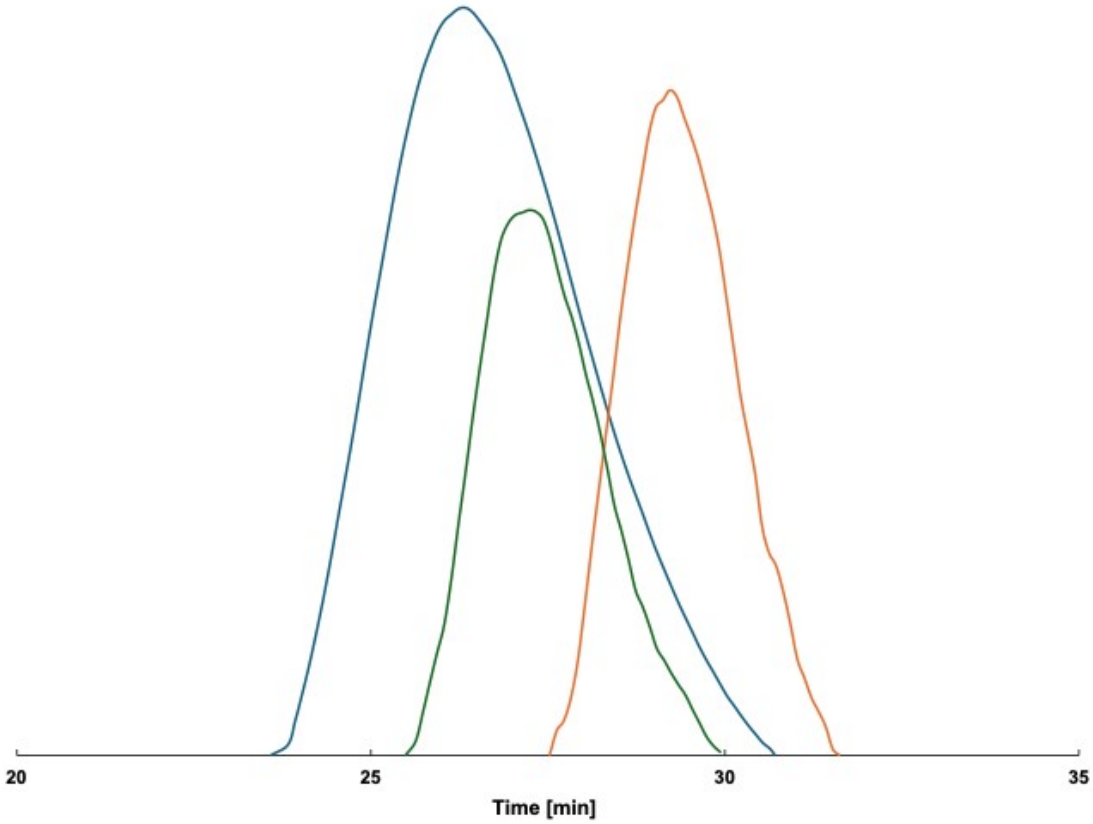

Figure S4. GPC chromatograms with relative retention time (dotted line) of P((HEMA-graft-LA_{12})-co-MAA)-b-P(EG_2MA-co-EG_8MA) (blue), P((HEMA-graft-LA_{12})-co-MAA) (green) and HEMA-graft-LA_{12} (orange) with an unimodal and narrow molecular weight distribution.

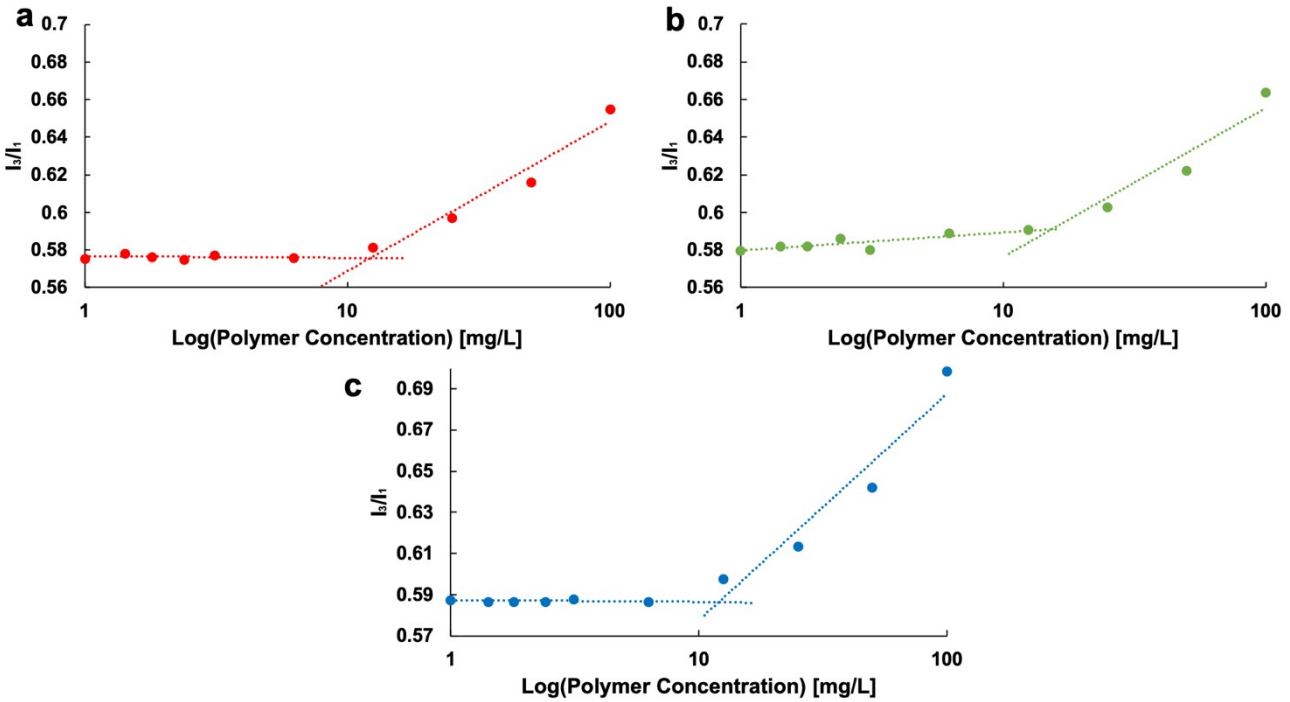

Figure S5. Determination of the CMC of nanoparticle formulations using pyrene as hydrophobic fluorescent probe. The ratio between the third and first vibronic emission peaks (I_3 = 384 nm/I_1 = 373 nm) is plotted as a function of the logarithm of polymer concentration. Each panel corresponds to a different formulation: (a) sample A (red circles), (b) sample B (green circles), (c) sample C (blue circles).

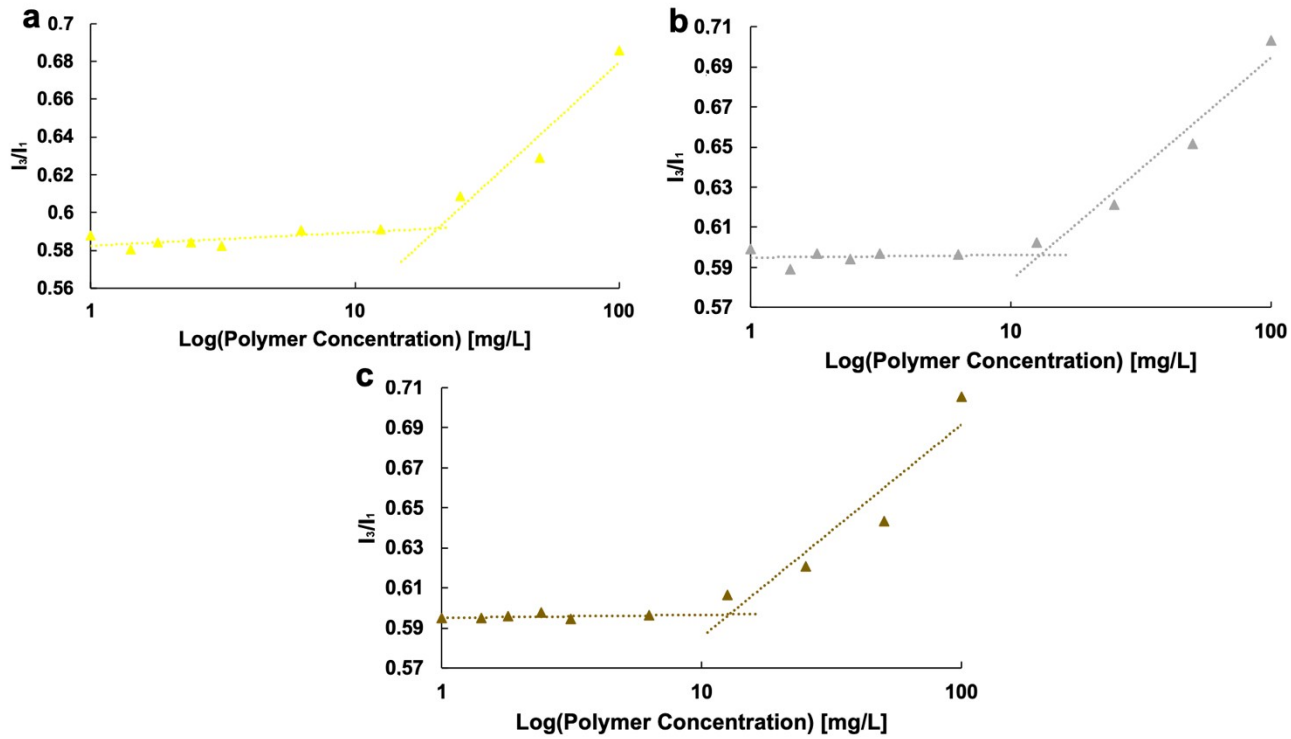

Figure S6. Determination of the CMC of nanoparticle formulations using pyrene as hydrophobic fluorescent probe. The ratio between the third and first vibronic emission peaks (I_3 = 384 nm/I_1 = 373 nm) is plotted as a function of the logarithm of polymer concentration. Each panel corresponds to a different formulation: (a) sample D (yellow triangles), (b) sample E (grey triangles), (c) sample F (brown triangles).

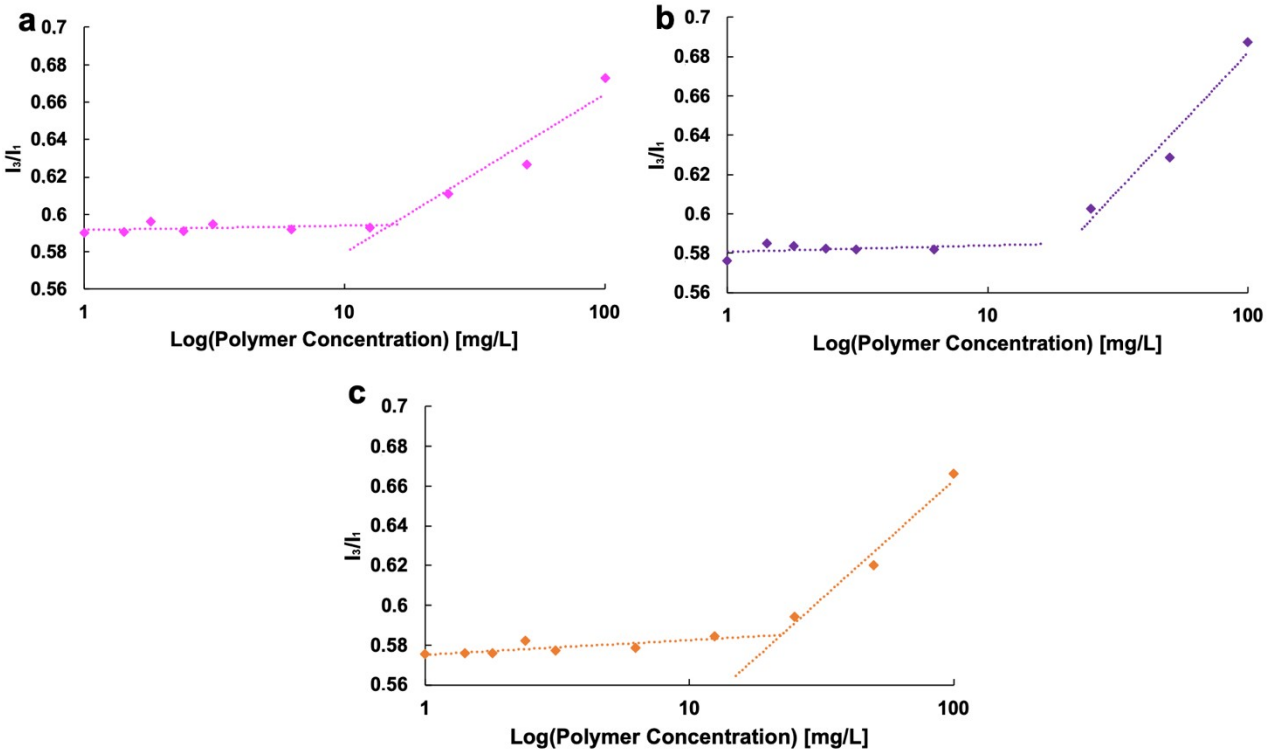

Figure S7. Determination of the CMC of nanoparticle formulations using pyrene as hydrophobic fluorescent probe. The ratio between the third and first vibronic emission peaks (I_3 = 384 nm/I_1 = 373 nm) is plotted as a function of the logarithm of polymer concentration. Each panel corresponds to a different formulation: (a) sample G (fuchsia diamond), (b) sample H (purple diamond), (c) sample I (orange diamond).

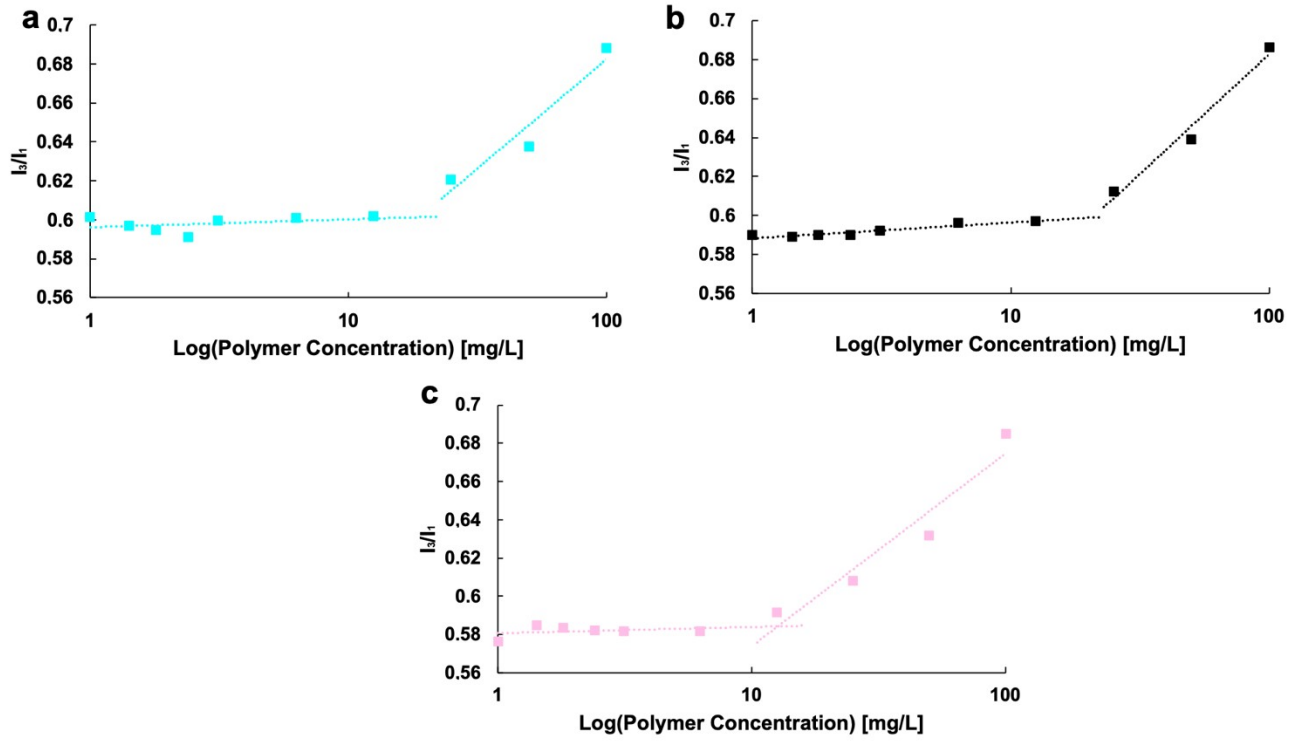

Figure S8. Determination of the CMC of nanoparticle formulations using pyrene as hydrophobic fluorescent probe. The ratio between the third and first vibronic emission peaks (I_3 = 384 nm/I_1 = 373 nm) is plotted as a function of the logarithm of polymer concentration. Each panel corresponds to a different formulation: (a) sample J (cyan square), (b) sample K (black square), (c) sample L (pink square).

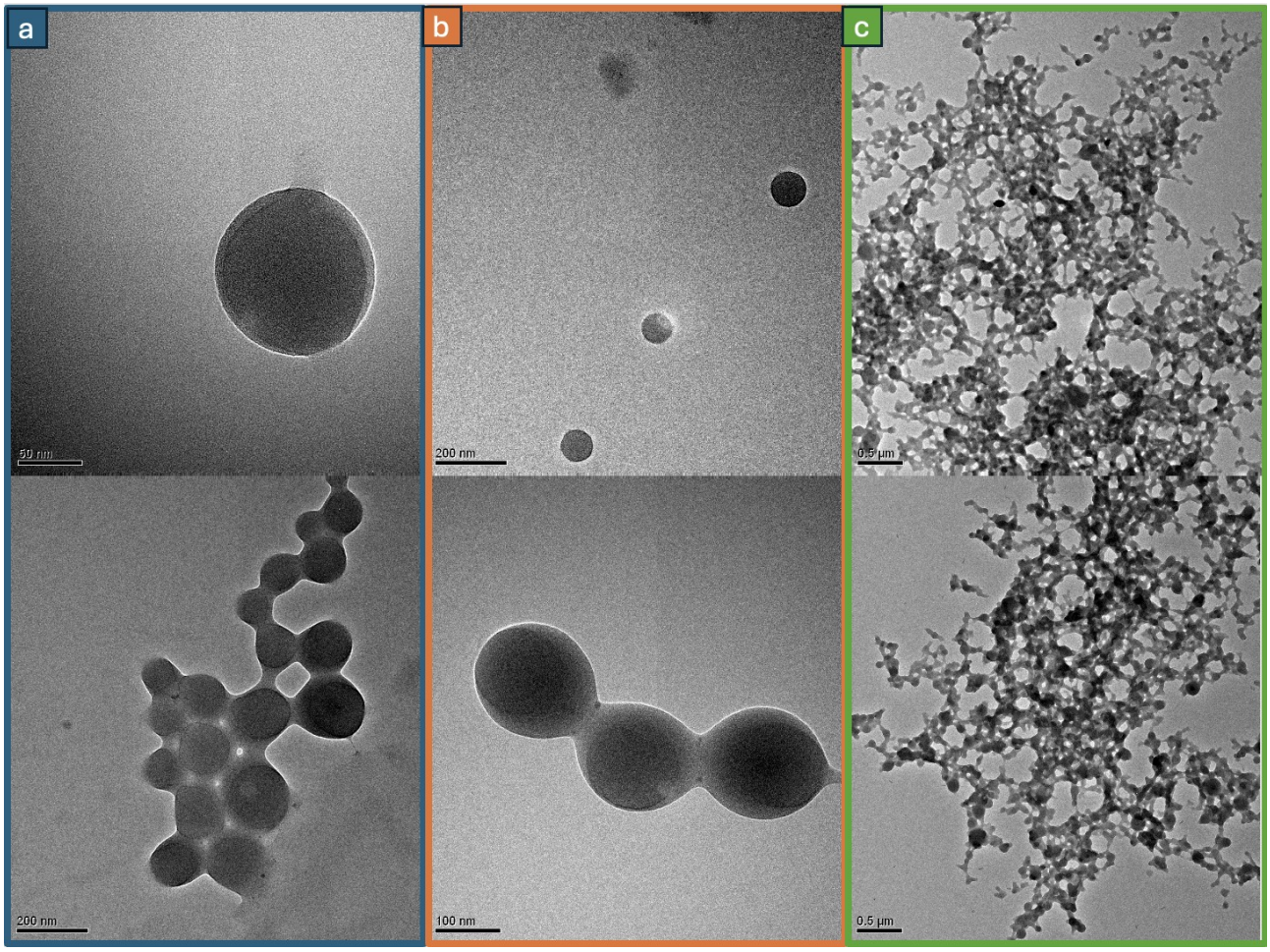

Figure S9. TEM images of representative nanoparticles prepared from sample E under different conditions: (a) room temperature, (b) after thermal treatment at 45 °C, and (c) after exposure to acidic conditions (pH 3). At room temperature, nanoparticles display a well-defined morphology. After thermal treatment, particles remain distinguishable, supporting the preservation of nanoparticle identity upon heating. Under acidic conditions, extended aggregated structures are observed, consistent with pH-induced colloidal destabilization.

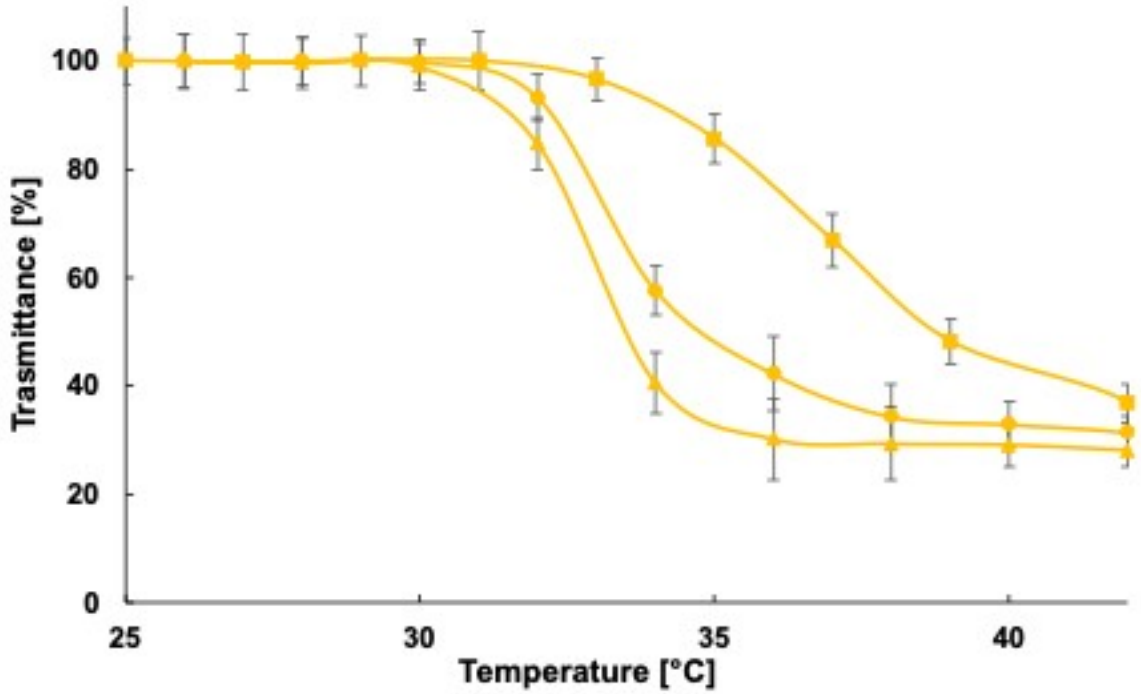

Figure S10. Temperature-dependent optical transmittance UV-vis of nanoparticle formulations J–L. A marked decrease in transmittance is observed above the critical temperature, indicating increased turbidity due to thermally induced nanoparticle aggregation. This behavior is consistent with the aggregation-driven increase in hydrodynamic diameter measured by DLS. Shape code: J (circles), K (squares), and L (triangles).

NMR-based calculation of monomer conversion and number-average molecular weight

The experimental degree of polymerization and the number-average molecular weight Mn of the HEMA-graft-LA_{12} macromonomer after ROP was estimated by ^{1}H NMR end-group analysis, using the integration ratio between the PLA methyl signal and the methacrylate vinyl proton signal (Figure S1) according to:

$$DP_{LA_{12}} = \frac{e_{peak\ area}}{a_{peak\ area}} + 1 \quad \text{(S1)}$$

$$Mn_{LA_{12}} = Mn_{HEMA} + Mn_{LA} \times DP_{LA_{12}} \quad \text{(S2)}$$

where Mn_{HEMA} and Mn_{LA} are the molecular weights of HEMA and lactic acid repeating units, respectively. $e_{peak\ area}$ and $a_{peak\ area}$ correspond to the integrated areas of peaks e and a, respectively, as indicated in Figure S1.

The experimental degrees of polymerization of HEMA-graft-LA_{12} and MAA in the first RAFT polymerization to synthesize P((HEMA-graft-LA_{12})-co-MAA) statistical copolymers, together with the corresponding number-average molecular weight, were calculated according to:

$$DP_{HEMA-graft-LA_{12}} = DP_{T-HEMA-LA_{12}} \times \chi_{HEMA-graft-LA_{12}} \quad \text{(S3)}$$

$$Mn_{HEMA-graft-LA_{12}} = Mn_{LA_{12}} \times DP_{HEMA-graft-LA_{12}} \quad \text{(S4)}$$

$$DP_{MAA} = DP_{T-MAA} \times \chi_{MAA} \quad \text{(S5)}$$

$$Mn_{MAA} = Mn_{MAA} \times DP_{MAA} \quad \text{(S6)}$$

$$Mn_{(HEMA-graft-LA_{12})-co-MAA} = Mn_{HEMA-graft-LA_{12}} + Mn_{MAA} \quad \text{(S7)}$$

Where $DP_{T\text{-}HEMA\text{-}LA_{12}}$ and $DP_{T\text{-}MAA}$ are the theoretical degrees of polymerization targeted from the monomer-to-CTA feed ratio for HEMA-graft-LA_{12} and MAA, respectively. $DP_{HEMA\text{-}graft\text{-}LA_{12}}$ and $DP_{MAA}$are the corresponding experimental degrees of polymerization calculated from the monomer conversions. $Mn_{LA_{12}}$ is the number-average molecular weight of the HEMA-graft-LA_{12} macromonomer determined by ^{1}H NMR end-group analysis (see Equation S2), Mn_{MAA} is the molecular weight of methacrylic acid, and Mn_{CTA} is the molecular weight of the RAFT agent.

$\chi_{HEMA\text{-}graft\text{-}LA_{12}}$ and χ_{MAA} are the fractional monomer conversions determined by ^{1}H NMR:

$$\chi_{HEMA-graft-LA_{12}} = \left(1 - \frac{a_{RED\ peak\ area\ t}}{e_{RED\ peak\ area\ t}}\right) \times 100 \quad \text{(S8)}$$

$$\chi_{MAA} = \left(1 - \frac{a_{BLUE\ peak\ area\ t}}{e_{BLUE\ peak\ area\ t}}\right) \times 100 \quad \text{(S9)}$$

Where $a_{RED\ peak\ area\ t}$ and $a_{BLUE\ peak\ area\ t}$ are the integrated areas of the characteristic vinyl proton signals of HEMA-graft-LA_{12} and MAA at time (t=24), respectively, and $e_{RED\ peak\ area\ t}$ and $e_{BLUE\ peak\ area\ t}$ are the integrated areas of the characteristic PLA methyl signal at time (t=24) (Figure S2). The corresponding conversion values are reported in Table 2.

The experimental degree of polymerization of the EGMA-based block was calculated according to:

$$DP_{EGMAn} = DP_{HEMA-graft-LA_{12}} \times DP_{LA_{12}} \times \left(\frac{g_{peak\ area\ t}}{2h_{peak\ area\ t}}\right) \quad \text{(S10)}$$

$$DP_{EG_8MA} = \frac{DP_{T-EG_8MA}}{DP_{T-EG_2MA} + DP_{T-EG_8MA}} \times DP_{EGMAn} \quad \text{(S11)}$$

$$DP_{EG_2MA} = \frac{DP_{T-EG_2MA}}{DP_{T-EG_2MA} + DP_{T-EG_8MA}} \times DP_{EGMAn} \quad \text{(S12)}$$

$$Mn_{EG_8MA} = Mn_{T-EG_8MA} \times DP_{EG_8MA} \quad \text{(S13)}$$

$$Mn_{EG_2MA} = Mn_{T-EG_2MA} \times DP_{EG_2MA} \quad \text{(S14)}$$

$$Mn_{EGMAn} = Mn_{EG_2MA} + Mn_{EG_8MA} \quad \text{(S15)}$$

Where $DP_{HEMA\text{-}graft\text{-}LA_{12}}$ is the degree of polymerization of HEMA-graft-LA_{12} units in the final copolymer, $DP_{LA_{12}}$ is the average number of lactic acid units per PLA graft, $g_{peak\ area\ t}$ is the integrated area of the EGMA ester methylene protons (4.02 ppm, -$COOCH_2$-)and $h_{peak\ area\ t}$ is the integrated area of the PLA methyl signal used as reference (Figure S3). The factor 2 accounts for the two protons of the EGMA ester methylene group. Because the resonances of EG_2MA and EG_8MA strongly overlap in the final copolymers, the individual contributions of the two monomers could not be reliably resolved by ^{1}H NMR.

Therefore, the total experimental degree of polymerization of the EGMA-based block was first calculated from the integrated EGMA signal, and the individual DP_{EG_2MA} and DP_{EG_8MA} values were then estimated by partitioning DP_{EGnMA} according to the theoretical DP of EG_2MA and EG_8MA in the feed ($DP_{T\text{-}EG_2MA}$ and $DP_{T\text{-}EG_8MA}$). $Mn_{T\text{-}EG_2MA}$ and $Mn_{T\text{-}EG_8MA}$ are the molecular weights of the monomers EG_2MA and EG_8MA. For the RAFT chain extension with EG_2MA and EG_8MA, the overall monomer conversion χ_{EGMAn} was calculated from the decrease of the methacrylate vinyl proton signal over time:

$$\chi_{EGMAn} = \left(1 - \frac{a_{peak\ area\ t}}{e_{peak\ area\ t}}\right) \times 100 \quad \text{(S16)}$$

Where $a_{peak\ area\ t}$ is the integrated area of the characteristic vinyl proton signal of EGMAn at time (t=24), and $e_{peak\ area\ t}$ are the integrated areas of the characteristic PLA methyl signal at time (t=24) (Figure S3). The corresponding conversion values are reported in Table 2.